

Photocatalytic Oxidation of Water by Silica-Supported Tris(4,4'-dialkyl-2,2'-bipyridyl)ruthenium Polymeric Sensitizers and Colloidal Iridium Oxide

Michikazu Hara, John T. Lean, and Thomas E. Mallouk*

Department of Chemistry, The Pennsylvania State University,
University Park, Pennsylvania 16802

Received May 16, 2001. Revised Manuscript Received September 6, 2001

A cationic polymer containing tris(4,4'-dialkyl-2,2'-bipyridyl)ruthenium groups linked by aliphatic spacers was studied as a photosensitizer for the catalytic oxidation of water in the presence of colloidal IrO₂. The polymer–colloidal IrO₂ system photocatalytically reduced persulfate, a sacrificial electron acceptor, and oxidized water to O₂ and H⁺ in solutions that were buffered at pH 6 by Na₂SiF₆ and NaHCO₃. The quantum efficiency for O₂ evolution and turnover number with respect to the Ru complex in the polymer reached 25% and 100, respectively. The polymer gradually aggregated in the Na₂SiF₆–NaHCO₃ buffer during the reaction, and this aggregation gradually decreased the photocatalytic activity of the system. Heterogeneous photosystems composed of this polymer and colloidal IrO₂ were also prepared using 70 nm diameter SiO₂ particles as supports. Photocatalysts made by the sequential loading of colloidal IrO₂ and the photosensitizer polymer onto SiO₂ particles at ca. pH 6 had much lower photocatalytic activity than did the unsupported system, presumably because there was little physical contact between the polymer and colloidal IrO₂ particles under these conditions. The most efficient heterogeneous photocatalyst was obtained by the adsorption of a mixture of the polymer and colloidal IrO₂ onto SiO₂ in Na₂SiF₆–NaHCO₃ solution. This composite had a high activity, comparable to that of the polymer–colloidal IrO₂ system. Transmission electron microscopy showed that the colloidal IrO₂ particles were covered with the polymer, which had aggregated in the solution. This result indicates that the polymer–IrO₂ aggregates retain their activity when immobilized on a support that might be used to organize overall water splitting systems.

Introduction

The goals of photocatalytic decomposition of water are to construct catalytic systems that split water into H₂ and O₂ under visible-light irradiation and to produce efficient photoconversion systems and devices for storing solar energy. Two basic approaches to these problems have emerged. One is to utilize wide band gap inorganic semiconductors as particles, single-crystal electrodes, or thin films. This approach has been investigated since the discovery of the Honda–Fujishima effect,¹ and there have been several reports of photocatalytic overall water splitting under UV irradiation.^{2–5} Another strategy is to use photosensitized systems that are responsive to visible light.^{6–8} In a previous paper, we reported light-

driven electron and energy transfer reactions in lamellar polyanion/polycation thin film supported on SiO₂ particles.⁹ The energy/electron transfer cascade consisted of sequentially adsorbed polyanions, polycations, and charged porphyrin molecules, interleaved with anionic Zr(HPO₄)₂·H₂O and HTiNbO₅ sheets. The overall energy/electron transfer quantum yield of the photosensitized cascade that was irradiated with visible light exceeded 50%. The next logical step toward a water splitting system would be to couple these photoredox cascades to dark catalysts for hydrogen and oxygen evolution in appropriate layers. One of the biggest stumbling blocks to the development of such integrated photosystems is the absence of an effective and stable oxygen evolution catalyst.

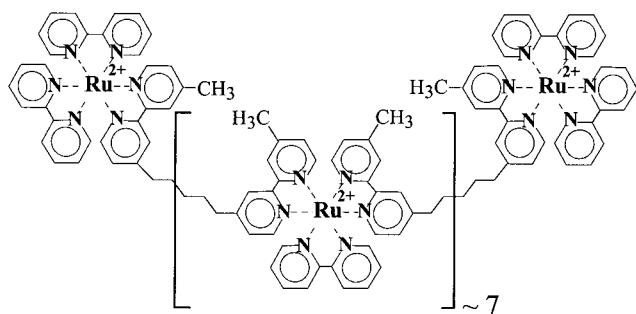
Tris(2,2'-bipyridyl)ruthenium [Ru(bpy)₃] is a particularly interesting sensitizer for visible-light water splitting.^{10–13} Visible light is absorbed by [Ru(bpy)₃]²⁺, forming an energetic and long-lived metal-to-ligand

* To whom correspondence should be addressed.

- (1) Fujishima, A.; Honda, K. *Nature* **1972**, *37*, 238.
- (2) Duonghong, D.; Borgarello, E.; Grätzel, M. *J. Am. Chem. Soc.* **1981**, *103*, 4685.
- (3) Domen, K.; Naito, S.; Onishi, T.; Tamaru, K.; Soma, M. *J. Phys. Chem.* **1982**, *86*, 3657.
- (4) Domen, K.; Kudo, A.; Shinozaki, A.; Tanaka, A.; Maruya, K.; Onishi, T. *J. Chem. Soc., Chem. Commun.* **1986**, 356.
- (5) Sayama, K.; Arakawa, H. *J. Chem. Soc., Chem. Commun.* **1992**, 150.
- (6) Kiwi, J.; Grätzel, M. *J. Am. Chem. Soc.* **1979**, *101*, 7214.
- (7) Kim, Y.; Salim, S.; Huq, M.; Mallouk, T. E. *J. Am. Chem. Soc.* **1991**, *113*, 9561.
- (8) (a) Kim, Y.; Atherton, S. J.; Brigham, E. S.; Mallouk, T. E. *J. Phys. Chem.* **1993**, *97*, 11802. (b) Saupé, G. B.; Kim, W.; Schmehl, R. H.; Mallouk, T. E. *J. Phys. Chem. B* **1997**, *101*, 2508.

- (9) Kaschak, D. M.; Lean, J. T.; Waraksa, C. C.; Saupé, G. B.; Mallouk, T. E. *J. Am. Chem. Soc.* **1999**, *121*, 3435.
- (10) Kiwi, J.; Grätzel, M. *Nature* **1979**, *285*, 657.
- (11) Harriman, A.; Richoux, M.; Christensen, P. A.; Moser, S.; Neta, P. *J. Chem. Soc., Faraday Trans. 1* **1987**, *83*, 3001.
- (12) Harriman, A.; Thomas, J. M.; Millward, G. R. *New J. Chem.* **1987**, *11*, 757.
- (13) Harriman, A.; Pickering, I. J.; Thomas, J. M.; Christensen, P. A. *J. Chem. Soc., Faraday Trans. 1* **1988**, *84*, 2795.

Scheme 1



charge transfer (MLCT) excited state. The complex in the MLCT state is oxidized to $[\text{Ru}(\text{bpy})_3]^{3+}$ by sacrificial acceptors such as $\text{S}_2\text{O}_8^{2-}$. Without an appropriate catalyst, no O_2 is formed and $[\text{Ru}(\text{bpy})_3]^{3+}$ is destroyed by nucleophilic attack of water and/or hydroxide ions. In the presence of a catalyst, which is typically a transition metal oxide, the photosensitizer is recycled and O_2 can be detected as a reaction product. The quantum yield for O_2 evolution reaches ca. 60% under optimal conditions. RuO_2 is an effective catalyst for O_2 evolution under these conditions, but its turnover number is typically small because of anodic corrosion. On the other hand, IrO_2 powder and colloidal IrO_2 ($\text{IrO}_2 \cdot x\text{H}_2\text{O}$) are known to be more stable and to have high activity as catalysts for O_2 evolution.¹¹ Colloidal IrO_2 is a favorable catalyst for our purposes because it possesses a negative charge at $\text{pH} > 2$.¹² Thus, colloidal IrO_2 is a reasonable candidate for insertion into lamellar energy/electron transfer cascades based on the sequential adsorption of oppositely charged sheets and polymers.

To study oxygen evolution in organized systems that might be adapted to overall photochemical water splitting, we synthesized a polymeric ruthenium tris(bipyridyl) sensitizer as shown in Scheme 1. This polymer should oxidize water to O_2 and H^+ photocatalytically in the presence of colloidal IrO_2 , provided there is good electronic contact between the $[\text{Ru}(\text{bpy})_3]^{2+}$ units in the polymer and the catalyst. In principle, because the polymer is cationic and the IrO_2 colloid is anionic in the pH range of interest, the two might function together as a photocatalytic unit for oxygen evolution. Further, the polymer- IrO_2 composite might be coupled to other charged surfaces to make more complex systems for photochemical water splitting. In this paper, we describe the photocatalytic oxidation of water by the polymer and colloidal IrO_2 dissolved in aqueous solutions (polymer-colloidal IrO_2 system) and heterogeneous photocatalysts that contain both the polymer and colloidal IrO_2 .

Experimental Section

Materials. Reagent grade $\text{AlCl}_3 \cdot 6\text{H}_2\text{O}$, Na_2SiF_6 , NaHCO_3 , $\text{Na}_2\text{S}_2\text{O}_8$, Na_2SO_4 , and sodium hydrogen citrate sesquihydrate were obtained from commercial sources. $[\text{Ru}(\text{bpy})_3]\text{Cl}_2 \cdot 6\text{H}_2\text{O}$ and potassium hexachloroiridate, K_2IrCl_6 , were used as received from Aldrich and Alfa, respectively. Spherical SiO_2 particles (70 nm diameter), which were used as supports, were available from earlier studies.¹⁴ The SiO_2 was heated in air at 550°C for 5 h to remove any adsorbed organic compounds.

(14) Egan, G. L.; Yu, J.-S.; Kim, C. H.; Lee, S. J.; Schaak, R. E.; Mallouk, T. E. *Adv. Mater.* **2000**, *12*, 1040.

Tris(4,4'-dialkyl-2,2'-bipyridyl)ruthenium Polymer. Dichlorotetrakis(dimethyl sulfoxide)ruthenium(II) and 1,5-bis(4'-methyl-2,2'-bipyridyl-4-yl)pentane were prepared according to literature methods.¹⁵ A 0.20 g (0.40 mmol) portion of $[\text{Ru}(\text{DMSO})_4\text{Cl}_2]$ and 0.17 g (0.40 mmol) of 1,5-bis(4'-methyl-2,2'-bipyridyl-4-yl)pentane were combined with 50 mL of chloroform and refluxed under argon for 1.5 h. The solvent was removed under reduced pressure to yield a dark brown oil. The oil was dissolved in a mixture of 10 mL of H_2O /15 mL of ethanol. A 0.10 g (0.64 mmol) portion of 2,2'-bipyridine was added, and the solution was refluxed for 2.5 h. A clear, bright orange-red solution resulted. The solvent was reduced to about 10 mL under reduced pressure, and the product was precipitated with aqueous ammonium hexafluorophosphate. The precipitate was filtered and washed with H_2O and diethyl ether to yield an orange powder (0.36 g, 95%). The degree of polymerization was determined from ^1H NMR experiments by assuming that the end groups contained two 2,2'-bipyridine units and the interior Ru^{2+} centers had one. The degree of polymerization can then be calculated from the ratio between the average peak areas for the 1,5-bis(4'-methyl-2,2'-bipyridyl-4-yl)pentane units and 2,2'-bipyridine units. The average degree of polymerization was determined by this method to be ca. 9. Anal. Calcd for $\text{C}_{326}\text{H}_{312}\text{F}_{108}\text{N}_{54}\text{P}_{18}\text{Ru}_9$ (found): C, 46.04% (46.33%); H, 3.70% (3.77%); 8.89% (8.88%). UV/vis (λ_{max} (nm), CH_3CN): 454 ($104\,000\ \text{M}^{-1}\ \text{cm}^{-1}$), 288 ($652\,000\ \text{M}^{-1}\ \text{cm}^{-1}$), 248 ($215\,000\ \text{M}^{-1}\ \text{cm}^{-1}$), 206 ($619\,000\ \text{M}^{-1}\ \text{cm}^{-1}$). ^1H NMR (δ (ppm), CD_3CN): 8.48 (m, bpy), 8.15 (m, Mebpy), 8.04 (m, bpy), 7.71 (s, bpy), 7.52 (m, Mebpy), 7.35 (m, bpy), 7.22 (s, Mebpy), 2.79 (s, $-\text{CH}_2-$), 2.52 (s, $-\text{CH}_3$), 1.73 (m, $-\text{CH}_2-$), 1.48 (m, $-\text{CH}_2-$). The PF_6^- salt of the polymer was converted to the Cl^- salt by dissolving the product in a minimum amount of acetonitrile and adding tetraethylammonium chloride in acetonitrile and a few drops of 12 M HCl. The Cl^- salt precipitates as a red film on the sides of the flask. Emission (λ_{max} (nm), H_2O): 620, excitation wavelength 460 nm. A 0.12 g portion of the solid polymer chloride salt was dissolved in 50 mL of deionized water, and the solution (2.7×10^{-4} M in polymer, 2.4×10^{-3} M in Ru-complex) was used to prepare the composites used in the photolysis experiments.

Synthesis of Colloidal IrO_2 . Colloidal IrO_2 ($\text{IrO}_2 \cdot x\text{H}_2\text{O}$) was obtained by the hydrolysis of solutions of hexachloroiridate (IrCl_6^{2-}).¹² A 0.030 g portion of K_2IrCl_6 (6.2×10^{-5} mol) was added to an aqueous solution of 0.05 g (1.9×10^{-4} mol) of sodium hydrogen citrate sesquihydrate which was dissolved in 50 mL of deionized water. The red-brown solution was adjusted to pH 7.5 with 0.25 M NaOH solution and was heated to 95°C in an oil bath with constant stirring. After being heated for 30 min, the solution was allowed to cool to room temperature and was adjusted to the initial pH with NaOH solution. The pH adjustment with NaOH and heating at 95°C for 30 min were repeated until the pH had stabilized at 7.5. The solution was then kept at 95°C for 2 h with oxygen bubbling through the solution in a round-bottom flask with a reflux condenser. The color of the solution became deep blue, signaling the formation of colloidal IrO_2 toward the end of the reaction.⁴ The colloidal IrO_2 solution was cooled to room temperature before being stirred with 10 mL of anion-exchange resin, DOWEX 2X8-50 (chloride form), to remove excess citrate ions. After 30 min, the resin was removed by filtration, and the final solution was diluted to 100 mL. The diameter of the colloidal particles was estimated to be ca. 10–20 nm by transmission electron microscopy (TEM). The citrate-stabilized colloidal IrO_2 solution was stable over a period of several months at this concentration.

Preparation of $\text{Al}_{13}\text{O}_4(\text{OH})_{24}(\text{H}_2\text{O})_{12}^{7+}$. The aluminum Keggin ion, $\text{Al}_{13}\text{O}_4(\text{OH})_{24}(\text{H}_2\text{O})_{12}^{7+}$, was prepared free of other Al species in soluble form by reaction of its sulfate salt with aqueous BaCl_2 .¹⁶ A 50 mL portion of an aqueous 0.25 M NaOH solution (12.5 mmol) was added dropwise to an aqueous

(15) (a) Evans, I. P.; Spencer, A.; Wilkinson, G. *J. Chem. Soc., Dalton Trans.* **1973**, 204. (b) Furue, M.; Yoshidzumi, T.; Kinoshita, S.; Kushida, T.; Nozakura, S.; Kamachi, M. *Bull. Chem. Soc. Jpn.* **1991**, *64*, 1632.

solution of 1.2 g of $\text{AlCl}_3 \cdot 6\text{H}_2\text{O}$ (5 mmol) in 50 mL of deionized water, and the solution was heated to 85 °C in an oil bath with constant stirring. After 20 min, 80 mL of aqueous 0.12 M Na_2SO_4 (10 mmol) was added to the clear Al^{3+} solution. The solution was kept at room temperature for 1 day to yield crystals of the sulfate salt $\text{NaAl}_3\text{O}_4(\text{OH})_{24}(\text{SO}_4)_4 \cdot x\text{H}_2\text{O}$. The crystals were separated by suction filtration, washed with deionized water, and dried. A 0.25 g portion of dry crystals was re-suspended in 100 mL of deionized water. A 0.28 g portion of $\text{BaCl}_2 \cdot 2\text{H}_2\text{O}$ (1.15 mmol) was added to this suspension, which was stirred for 4 h and diluted to 250 mL (ca. 7×10^{-4} M $\text{Al}_3\text{O}_4(\text{OH})_{24}(\text{H}_2\text{O})_{12}^{7+}$). The BaSO_4 produced in the reaction was removed by filtration and centrifugation.

Supported Polymer/Catalyst Materials. Two kinds of heterogeneous photocatalysts were made by loading the sensitizer polymer and colloidal IrO_2 onto spherical SiO_2 support particles. In both cases, the polymer was adsorbed onto the supports at pH 5.5–5.8 because the subsequent photolysis reaction was carried out in that pH range.

A. Polymer/ IrO_2 /Keggin/ SiO_2 . Colloidal IrO_2 particles were adsorbed onto the anionic SiO_2 support by means of an intermediate layer of cationic aluminum Keggin ions ($\text{IrO}_2/\text{Keggin}/\text{SiO}_2$), and the cationic Ru-polymer was then adsorbed onto $\text{IrO}_2/\text{Keggin}/\text{SiO}_2$. Keggin ions were first adsorbed on the spherical SiO_2 particles by stirring 0.05–0.10 g of SiO_2 in 5.6 mL of 7×10^{-4} M $\text{Al}_3\text{O}_4(\text{OH})_{24}(\text{H}_2\text{O})_{12}^{7+}$ solution. After being stirred for 3 h, the mixture was centrifuged, and the Keggin-adsorbed SiO_2 ($\text{Keggin}/\text{SiO}_2$) sample was rinsed three times in deionized water. During each rinse the suspension was stirred vigorously for 30 min and then centrifuged to collect the solid. The solid $\text{Keggin}/\text{SiO}_2$ sample was suspended in 10 mL of deionized water and stirred for 2 h after 0.01–30 mL of 6.2×10^{-4} M colloidal IrO_2 solution was added to the suspension. The IrO_2 -deposited $\text{Keggin}/\text{SiO}_2$ ($\text{IrO}_2/\text{Keggin}/\text{SiO}_2$) sample was collected after being rinsed as described above and was re-suspended in 3 mL of deionized water. The amount of colloidal IrO_2 adsorbed onto the $\text{Keggin}/\text{SiO}_2$ support was estimated in each case by measuring the 500–700 nm absorbance of the supernatant rinse solutions. Colloidal IrO_2 has a broad absorption band in the range of 500–700 nm.¹² These measurements showed that 0.1 g of $\text{Keggin}/\text{SiO}_2$ could adsorb a maximum loading of 4.2×10^{-6} mol of colloidal IrO_2 . Polymer/ IrO_2 /Keggin/ SiO_2 samples were prepared by the addition of 10 mL of the polymer-containing solution to 3 mL of the $\text{IrO}_2/\text{Keggin}/\text{SiO}_2$ suspension. Two different polymer solutions were used: one in which the pH was adjusted to 5.5–5.8 by addition of 10^{-5} M HCl and one which was buffered at the same pH by using Na_2SiF_6 – NaHCO_3 solution (Na_2SiF_6 , 2.2×10^{-2} M; NaHCO_3 , 2.8×10^{-2} M). After being stirred for 3 h, the unbuffered and buffered samples were centrifuged and rinsed with water adjusted to pH 5.5 with dilute HCl or with Na_2SiF_6 – NaHCO_3 buffer, respectively, until there was no detectable UV–vis absorbance (460 nm) of the polymer in the supernatant rinse solutions. The loading of the polymer was controlled by adjusting the polymer concentration (1.0 – 3.0×10^{-5} M on a monomer basis) used in the adsorption step, and the resulting loading was determined by measuring the 460 nm absorbance of the supernatant rinse solutions.

As a control experiment, underivatized SiO_2 was stirred in a colloidal IrO_2 solution prior to the adsorption of Keggin ions. In this case, colloidal IrO_2 was not detectably adsorbed onto SiO_2 . A second set of control experiments were done to determine whether the Ru-containing polymer required IrO_2 for adsorption onto the silica support. In both the unbuffered and buffered solutions, there was no observable difference ($\pm 10\%$) in the amount of polymer adsorbed onto $\text{IrO}_2/\text{Keggin}/\text{SiO}_2$ and $\text{Keggin}/\text{SiO}_2$ supports. Taken together, these control experiments show that while the presence of the cationic Keggin ion is required for adsorption of anionic IrO_2 onto the anionic silica support, the anionic IrO_2 particles have little or no role in binding the cationic Ru-containing polymer to the support.

B. Polymer– IrO_2 / SiO_2 . In this case, a solution of the cationic Ru-containing polymer and anionic colloidal IrO_2 was made and then adsorbed onto the silica particles. A 0.5 mL portion of 6.2×10^{-4} M colloidal IrO_2 solution (3.1×10^{-7} mol) and 0.1–1.0 mL of the polymer solution (2.4×10^{-3} M on a monomer basis) were added to 10 mL of the unbuffered or buffered pH 5.5–5.8 solutions described above. SiO_2 (0.05–0.10 g) was then immediately stirred into the solutions. After 1 h, the polymer– $\text{IrO}_2/\text{SiO}_2$ samples were centrifuged and rinsed as described above.

Photocatalytic Oxidation of Water. Oxygen evolution was measured from photolysis of the monomeric tris(2,2'-bipyridyl)ruthenium complex ($[\text{Ru}(\text{bpy})_3]^{2+}$) in the presence of colloidal IrO_2 , from the Ru-containing polymer in the presence of colloidal IrO_2 , and from the heterogeneous photocatalysts A and B described above. All experiments were done using persulfate as a sacrificial electron acceptor in a Pyrex test tube reactor (36.5 mL total volume). The reactor was sealed with a silicone rubber septum and was enclosed in an outer Pyrex chamber with a rubber septum, with Ar flowing through the outer chamber in order to prevent atmospheric contamination of the inner reactor. The solutions were adjusted to pH 5.5–5.8 by using NaOH, KH_2PO_4 – $\text{Na}_2\text{B}_4\text{O}_7$, or Na_2SiF_6 – NaHCO_3 solutions. The total volume of the solution in the inner reactor was 5 mL, and the concentrations of $\text{Na}_2\text{S}_2\text{O}_8$ and Na_2SO_4 were 1.0×10^{-2} (50 mmol/5 mL) and 5.0×10^{-2} M, respectively. For O_2 evolution from the heterogeneous photocatalysts, 0.05–0.10 g of the catalysts (which contained 6.2×10^{-5} M colloidal IrO_2) were suspended in 5 mL of a solution composed of 5.0×10^{-2} M Na_2SiF_6 – NaHCO_3 (Na_2SiF_6 , 2.2×10^{-2} M; NaHCO_3 , 2.8×10^{-2} M), Na_2SO_4 (1.0×10^{-2} M), and $\text{Na}_2\text{S}_2\text{O}_8$ (5.0×10^{-2} M). The pH of the solution before reaction was 5.5–5.7. After being purged with Ar, the solutions were irradiated with constant stirring with a 300 W Xe lamp equipped with a 450 ± 20 nm interference filter. The gas accumulated in the dead volume of the reactor was withdrawn by a sample-lock syringe and was analyzed by gas chromatography using a thermal conductivity detector and Molecular Sieve 5A packed columns (Supelco) held at ambient temperature. Air contamination, which could be detected as a nitrogen signal, was not observed. When the sacrificial acceptor was exhausted after photolysis, the reaction was resumed after 50 μmol of $\text{Na}_2\text{S}_2\text{O}_8$ was added to the reactor and the pH of the solution was restored to the initial value by the addition of NaHCO_3 .

Results and Discussion

Photochemical Oxygen Evolution from Ru Complex–Colloidal IrO_2 and Polymer–Colloidal IrO_2 .

Figure 1 compares the time course of O_2 evolution from polymer–colloidal IrO_2 and $[\text{Ru}(\text{bpy})_3]^{2+}$ –colloidal IrO_2 photosystems. The concentrations of the polymer, monomeric ($[\text{Ru}(\text{bpy})_3]^{2+}$), and colloidal IrO_2 were 1.2×10^{-5} (1.1×10^{-4} M on a monomer basis), 1.1×10^{-4} , and 6.2×10^{-5} M, respectively. The pH of the solution before and after reaction is inset in the figure. The O_2 yield for the polymer–colloidal IrO_2 system in an unbuffered NaOH-containing solution was very low, and the pH fell rapidly during the reaction. In the unbuffered solution, the pH drops rapidly because the reaction produces H^+ , and at low pH, the thermodynamic driving force for O_2 evolution from $[\text{Ru}(\text{bpy})_3]^{3+}$ is reduced. O_2 evolution in $[\text{Ru}(\text{bpy})_3]^{2+}$ –catalyst systems is known to proceed most efficiently in a narrow pH range around 5–6.¹¹ When the polymer–colloidal IrO_2 system photolysis was carried out in a buffered solution (pH 5.8) with conventional phosphate buffer (KH_2PO_4 , 7.2×10^{-2} M; $\text{Na}_2\text{B}_4\text{O}_7$, 2.9×10^{-3} M), the pH was almost constant during light irradiation but no oxygen was detected. This is consistent with our previous observations that phosphate accelerates the decomposition of Ru-complex sensitizers.¹⁷

(16) Johansson, G.; Lundgren, G.; Sillen, L. G.; Soderquist, R. *Acta Chem. Scand.* **1960**, 769.

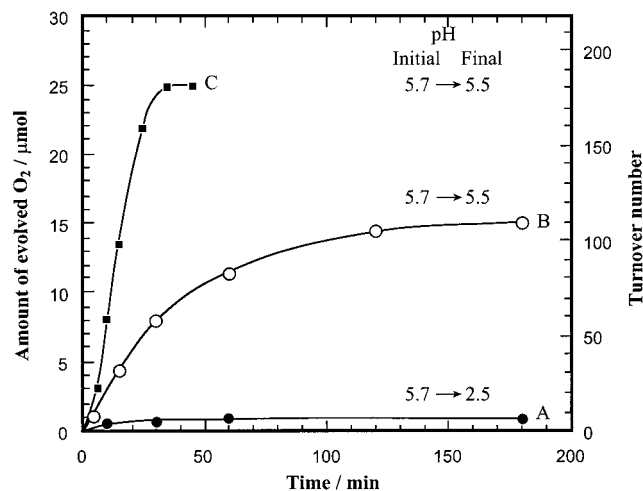


Figure 1. Time course of O_2 evolution from polymer-colloidal IrO_2 and $[Ru(bpy)_3]^{2+}$ -colloidal IrO_2 photosystems under visible-light irradiation ($\lambda = 450 \pm 20$ nm): A, polymer-colloidal IrO_2 photosystem in a solution adjusted at pH 5.7 by NaOH; B, polymer-colloidal IrO_2 photosystem in a Na_2SiF_6 - $NaHCO_3$ buffer-containing solution; C, $[Ru(bpy)_3]^{2+}$ -colloidal IrO_2 photosystem in the Na_2SiF_6 - $NaHCO_3$ buffer-containing solution; solution, 5.0 mL; polymer, 1.4×10^{-5} M (1.1×10^{-4} M on a monomer basis); $[Ru(bpy)_3]^{2+}$, 1.1×10^{-4} M; colloidal IrO_2 , 6.2×10^{-5} M; $Na_2S_2O_8$, 1.0×10^{-2} M; Na_2SO_4 , 5.0×10^{-2} M; Na_2SiF_6 - $NaHCO_3$ buffer, 5.0×10^{-2} M (Na_2SiF_6 , 2.2×10^{-2} M; $NaHCO_3$, 2.8×10^{-2} M).

In a solution containing Na_2SiF_6 and $NaHCO_3$ (Na_2SiF_6 , 2.2×10^{-2} M; $NaHCO_3$, 2.8×10^{-2} M), oxygen was evolved from polymer-colloidal IrO_2 solutions and the total turnover number exceeded 100. The initial quantum efficiency for O_2 evolution was estimated to be ca. 25% from the rate of O_2 evolution ($0.32 \mu\text{mol min}^{-1}$) at the early stage of reaction (5–15 min) and the incident photon flux. The pH of the solution was almost constant during reaction as shown in Figure 1. This behavior is consistent with our previous observations of $[Ru(bpy)_3]^{2+}$ photolysis in the same buffer.¹⁷ Figure 2 correlates oxygen evolution activity with the concentration of the Ru-containing polymer. The rates were measured at the early stage of reaction (5–15 min). The turnover number reaches a maximum as the rate of O_2 evolution reaches a plateau at a polymer concentration of 1.0 – 1.4×10^{-5} M. At low polymer concentration, the incident light is not efficiently absorbed and the oxygen evolution rate is near zero. Both the rate of oxygen evolution and the turnover number increase with increasing polymer concentration, suggesting that oxygen evolution only occurs when the polymer molecules are adsorbed on the colloid. Similar behavior was found for the monomeric $[Ru(bpy)_3]^{2+}$ sensitizer.¹⁷ Beyond 1.0 – 1.4×10^{-5} M concentration, the background hydrolysis rate exceeds the rate of oxygen evolution and the turnover number decreases. This drop in turnover number is consistent with the idea that at high polymer concentration a larger fraction of the $[Ru(bpy)_3]^{2+}$ sensitizer is photo-oxidized but is not involved in oxygen evolution, because it does not have access to the IrO_2 catalyst surface.

The Ru-containing polymer aggregated gradually during the reaction, as evidenced by the fact that it

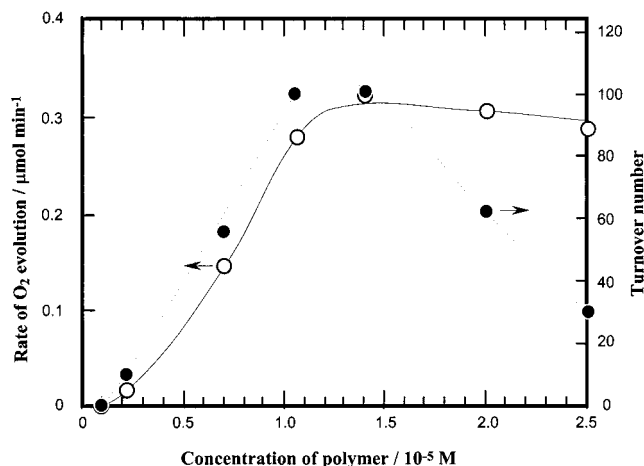


Figure 2. Dependence of the photocatalytic activity of polymer-colloidal IrO_2 system on the concentration of the polymer; colloidal IrO_2 , 6.2×10^{-5} M; $Na_2S_2O_8$, 1.0×10^{-2} M; Na_2SO_4 , 5.0×10^{-2} M; Na_2SiF_6 - $NaHCO_3$ buffer, 5.0×10^{-2} M.

precipitated from a quiescent solution, and the Na_2SiF_6 - $NaHCO_3$ buffer was found to accelerate this process. When 5 mL of Na_2SiF_6 - $NaHCO_3$ solution (Na_2SiF_6 , 2.2×10^{-2} M; $NaHCO_3$, 2.8×10^{-2} M) containing 1.4×10^{-5} M polymer was stirred in the dark, the amount of aggregated polymer that precipitated increased with stirring time and reached ca. 70% of the polymer in the solution (4.9×10^{-8} mol) after 3 h of stirring. Further stirring did not increase the amount of aggregated polymer. Neither the Na_2SiF_6 solution nor the $NaHCO_3$ solution precipitated the polymer, and a Na_2SiF_6 - $Na_2B_4O_7$ solution at pH 5.7 (Na_2SiF_6 , 2.6×10^{-2} M; $Na_2B_4O_7$, 0.11 M) aggregated the polymer as well as the Na_2SiF_6 - $NaHCO_3$ solution; therefore, the aggregation is attributed to a reaction between Na_2SiF_6 and the base. Silicic acid, H_2SiO_3 , or colloidal silica formed by the hydrolysis of Na_2SiF_6 are likely candidates for the aggregation of the cationic polymer, because both should be polyanions at pH 5.5–5.8.¹⁸ The aggregation of the polymer in the Na_2SiF_6 - $NaHCO_3$ solution was not entirely irreversible. A rinse with 20 mL of 10^{-5} M HCl solution (pH 5.7) dissolved ca. 70% of the above aggregated polymer (3.2×10^{-8} mol) in the rinse solution.

The polymer-colloidal IrO_2 system had a lower photocatalytic activity than the monomeric $[Ru(bpy)_3]^{2+}$ -colloidal IrO_2 system under the same conditions. As shown in Figure 1, 25 μmol of O_2 was evolved from the latter system without any decrease in activity.¹⁷ This value corresponds to the stoichiometric amount of O_2 that can be evolved from the sacrificial acceptor. Monomeric $[Ru(bpy)_3]^{2+}$ was not aggregated during the reaction, and no precipitate was found after stirring the solution in dark for 1 day. It is probable that the aggregation of the polymer causes the difference in activity between both systems. In the aggregated state, not all of the Ru subunits of the polymer are within electron transfer distance of the colloidal catalyst.

To examine the effects of aggregation of the polymer, $[Ru(bpy)_3]^{2+}$ -colloidal IrO_2 and polymer-colloidal IrO_2

(17) Hara, M.; Waraksa, C. C.; Lean, J. T.; Lewis, B. A.; Mallouk, T. E. *J. Phys. Chem. A* **2000**, *104*, 5275.

(18) Mellor, J. W. *A Comprehensive Treatise on Inorganic and Theoretical Chemistry*; Longmans, Green and Co.: London, 1925; p 943.

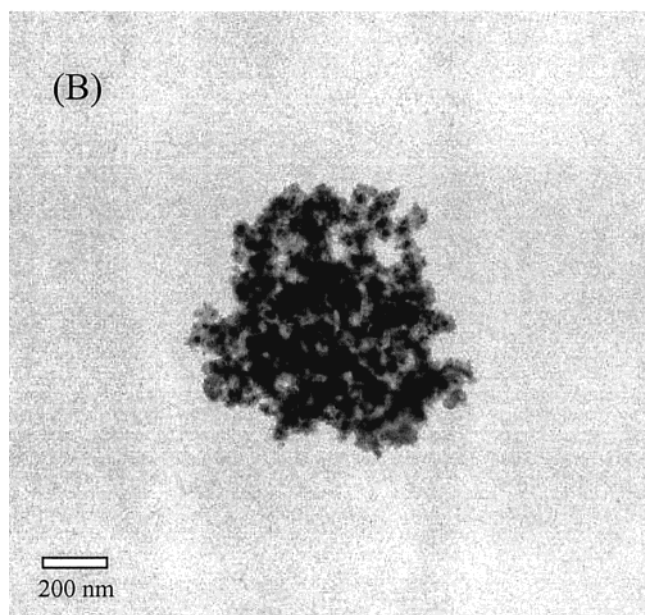
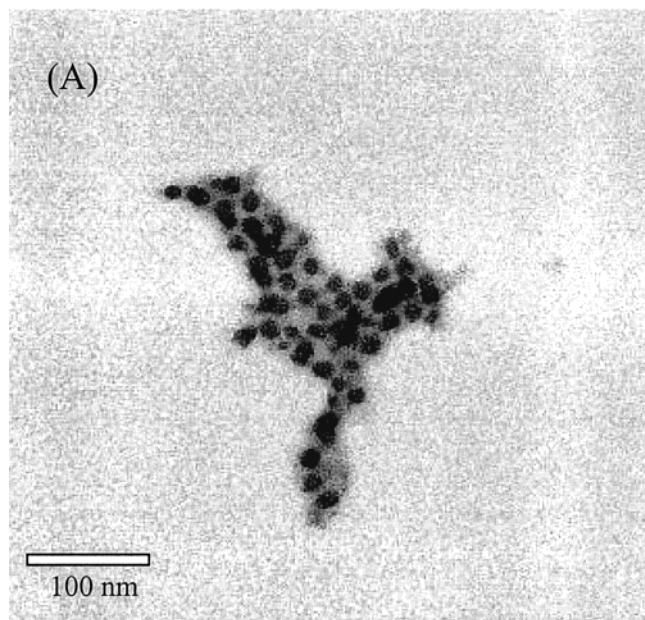


Figure 3. TEM images of colloidal IrO₂ and aggregated polymer with colloidal IrO₂: A, colloidal IrO₂; B, polymer and colloidal IrO₂ aggregated in Na₂SiF₆-NaHCO₃ solution.

solutions were irradiated with light after being allowed to stand for 1–5 h in dark before reaction. The aging period before reaction did not influence the activity of [Ru(bpy)₃]²⁺, while the activity of the polymer solution decreased substantially with time. Aging for 3 h reduced the rate of evolution and total turnover number to ca. 1/10th of their values under optimized conditions. Figure 3 shows TEM images of colloidal IrO₂ and an aggregated polymer sample. The aggregated sample was obtained by stirring a Na₂SiF₆-NaHCO₃ solution containing the polymer–colloidal IrO₂ system for 3 h, followed by centrifugation and rinsing with dilute HCl solution at pH 5.7 as described above. In this sample, colloidal IrO₂ particles of 10–20 nm diameter and the polymer are aggregated together.

Supported Polymer/IrO₂ Photocatalysts. To overcome problems associated with the aggregation of

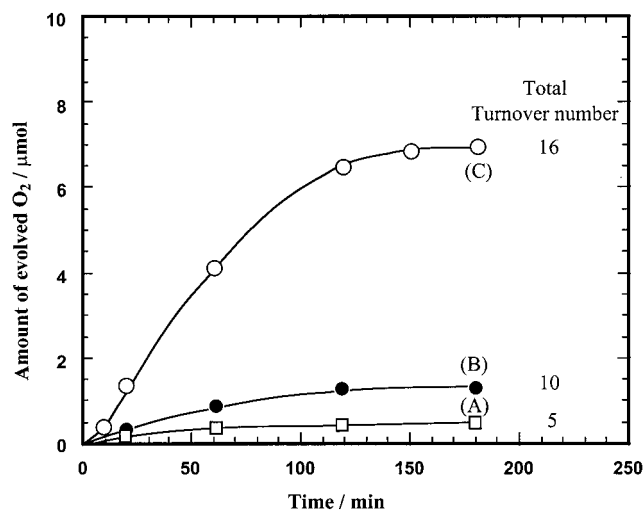


Figure 4. Time course of O₂ evolution from polymer/IrO₂/Keggin/SiO₂ sample; SiO₂, 0.05 g; IrO₂, 3.1 × 10⁻⁷ mol. The amount of adsorbed polymer: A, 3.0 × 10⁻⁸ mol; B, 6.3 × 10⁻⁸ mol; C, 2.2 × 10⁻⁷ mol.

polymer–colloidal IrO₂ photocatalysts, we prepared composites in which these components were immobilized on spherical silica particles. These silica particles serve as a model for more complex anionic supports, such as layered metal oxide semiconductors, which might be used to couple the oxygen evolution reaction to photocatalytic hydrogen evolution.^{7,8} To couple the polymer and IrO₂ to anionic silica, two approaches were tried. In one, cationic aluminum Keggin ions (Al₁₃O₄(OH)₂₄(H₂O)₁₂⁷⁺) were first adsorbed to make the silica surface cationic. The IrO₂ colloid and sensitizer polymer were then sequentially adsorbed. In the other approach, the cationic polymer/IrO₂ composite was directly adsorbed on the anionic silica surface. The structure and catalytic activity of these composites were then compared.

Oxygen Evolution from Polymer/IrO₂/Keggin/SiO₂. The polymer/IrO₂/Keggin/SiO₂ samples prepared in dilute HCl solution had no photocatalytic activity for oxidation of water. The largest amount of adsorbed polymer on an IrO₂/Keggin/SiO₂ substrate (IrO₂, 3.1 × 10⁻⁷ mol; SiO₂, 0.10 g) was 5.8 × 10⁻⁹ mol (5.2 × 10⁻⁸ mol on a monomer basis). When 3.1 × 10⁻⁷ mol of colloidal IrO₂ was deposited onto 0.05–0.10 g of SiO₂, the maximum loading of the polymer increased in proportion to SiO₂ support, indicating that most of the polymer is not adsorbed on the colloidal IrO₂ particles but on the SiO₂ support itself. The water oxidation reaction becomes more efficient with increasing addition of the polymer to the solution. However, the polymer adsorbed onto IrO₂/Keggin/SiO₂ in an unbuffered solution does not oxidize water, presumably because little or none of it is in physical contact with IrO₂.

To increase the polymer loading on the IrO₂/Keggin/SiO₂ supports, the latter was stirred with a Na₂SiF₆-NaHCO₃ solution containing the polymer. In this case, IrO₂/Keggin/SiO₂ adsorbs the polymer aggregated by base hydrolysis of Na₂SiF₆. Figure 4 shows the time course of O₂ evolution from these samples. The amounts of SiO₂ support and deposited IrO₂ were 0.05 g and 3.1 × 10⁻⁷ mol, respectively. Total turnover numbers with respect to the monomeric Ru complex in the polymer are inset in the figure. The sample at 2.2 × 10⁻⁷ mol

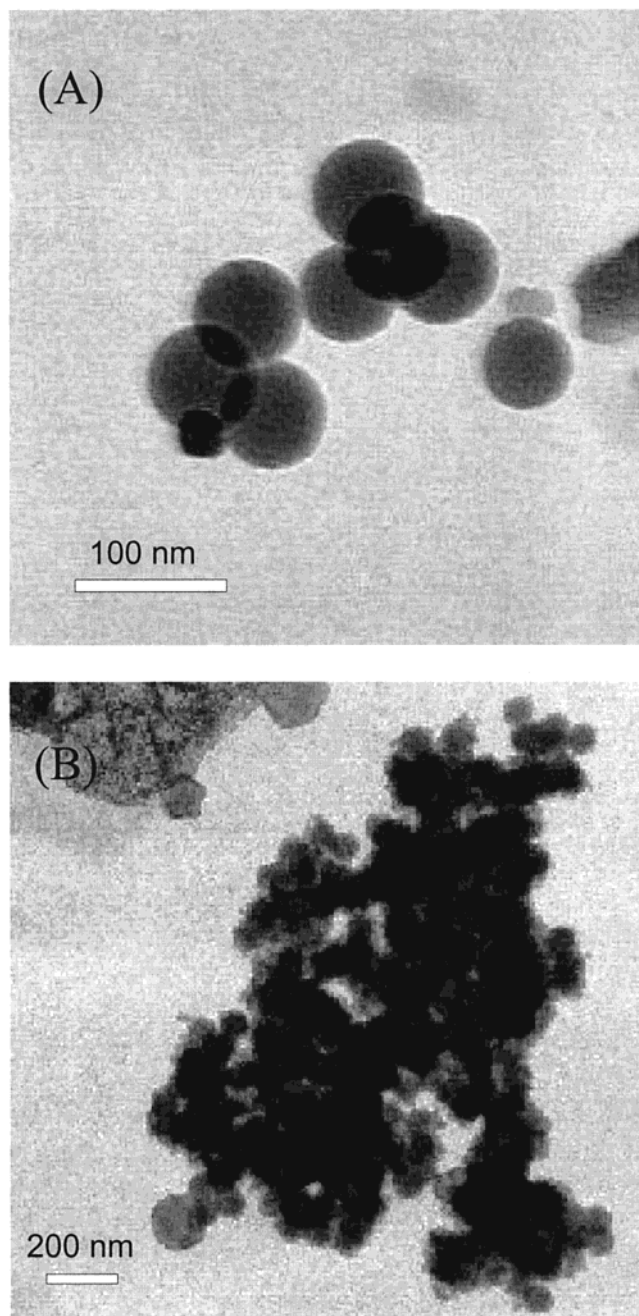


Figure 5. TEM images of IrO₂/Keggin/SiO₂ and polymer/IrO₂/Keggin/SiO₂ samples: SiO₂, 0.05 g; IrO₂, 3.1 × 10⁻⁷ mol; polymer, 2.2 × 10⁻⁷ mol.

(1.8 × 10⁻⁶ mol monomer), which was the maximum loading of the polymer under these conditions, had the highest activity among the polymer/IrO₂/Keggin/SiO₂ samples (IrO₂, 5.0 × 10⁻⁸ to 1.1 × 10⁻⁶ mol; SiO₂, 0.05 g). The amount of loaded polymer corresponded to ca. 70 times that in unbuffered dilute HCl solution and was larger than the total amount of the polymer in the polymer-colloidal IrO₂ system (7.0 × 10⁻⁸ mol in 5 mL (1.4 × 10⁻⁵ M)). TEM images of the IrO₂/Keggin/SiO₂ and polymer/IrO₂/Keggin/SiO₂ samples under the optimal conditions are shown in Figure 5. A colloidal IrO₂ particle of 20 nm diameter is attached to a 70 nm diameter SiO₂ particle through Keggin ions on IrO₂/Keggin/SiO₂, and the TEM image of polymer/IrO₂/Keggin/SiO₂ shows that the substrate is covered with

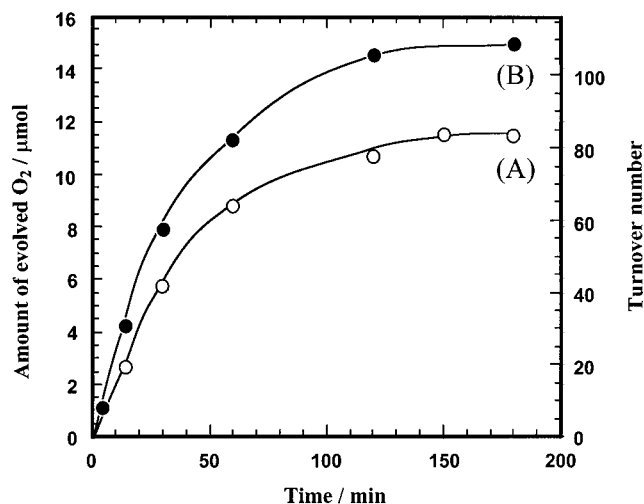


Figure 6. Time course of O₂ evolution from polymer-IrO₂/SiO₂ system: A, polymer-IrO₂/SiO₂ sample (polymer, 6.9 × 10⁻⁸ mol; IrO₂, 3.1 × 10⁻⁷ mol; SiO₂, 0.05 g); B, polymer-colloidal IrO₂ sample (polymer, 1.4 × 10⁻⁵ M (2.2 × 10⁻⁷ mol); colloidal IrO₂, 6.2 × 10⁻⁵ M (3.1 × 10⁻⁷ mol)).

aggregated polymer. These results show that while the aggregated polymer is bound to the support, the activity is quite small compared to that of the unsupported polymer-colloidal IrO₂ system.

Photocatalytic Oxidation of Water by Polymer-IrO₂/SiO₂. Polymer-IrO₂/SiO₂ samples (SiO₂, 0.04 g) prepared in dilute HCl solution showed low oxygen evolution activity even under optimized conditions. The highest rate of O₂ evolution and total turnover number were obtained with a maximum loading of the polymer (2.8 × 10⁻⁸ mol) and 8.1 × 10⁻⁷ mol of colloidal IrO₂ but were only 0.01 μmol min⁻¹ and 10, respectively.

On the other hand, the preparation of similar composites in a Na₂SiF₆-NaHCO₃ solution resulted in efficient photocatalysts. Figure 6 compares the time course of O₂ evolution from a polymer-IrO₂/SiO₂ sample prepared in Na₂SiF₆-NaHCO₃ solution (polymer, 6.9 × 10⁻⁸ mol; and IrO₂, 3.1 × 10⁻⁷ mol) to that from a polymer-colloidal IrO₂ sample (polymer, 6.9 × 10⁻⁸ mol; colloidal IrO₂, 3.1 × 10⁻⁷ mol). The quantum efficiency for O₂ evolution and total turnover number reached 20% and 80, respectively, which were somewhat lower than those of the polymer-colloidal IrO₂ system. There was no noticeable difference in activity before and after the sample had been allowed to stand for 5 h prior to reaction, indicating that the silica support stabilizes the polymer/IrO₂ composite against further aggregation. A TEM image of the polymer-IrO₂/SiO₂ sample is shown in Figure 7. The dark spots on the SiO₂ particles covered with the aggregated polymer have the diameter that was expected for colloidal IrO₂ particles, implying that the anionic SiO₂ particles adsorb dispersed IrO₂ particles covered by the cationic polymer. Figures 8 and 9 correlate the photocatalytic activity with the amounts of the adsorbed polymer and SiO₂, respectively, and show that the highest activity is obtained by loading 6.9 × 10⁻⁸ mol of the polymer and 3.1 × 10⁻⁷ mol of colloidal IrO₂ onto 0.04 g of SiO₂. Although the preparation in Na₂SiF₆-NaHCO₃ solution can increase the loading of the polymer on the SiO₂ support, the adsorption of more polymer than 6.9 × 10⁻⁸ mol reduced the activity. This is possibly due to an inner filter of light

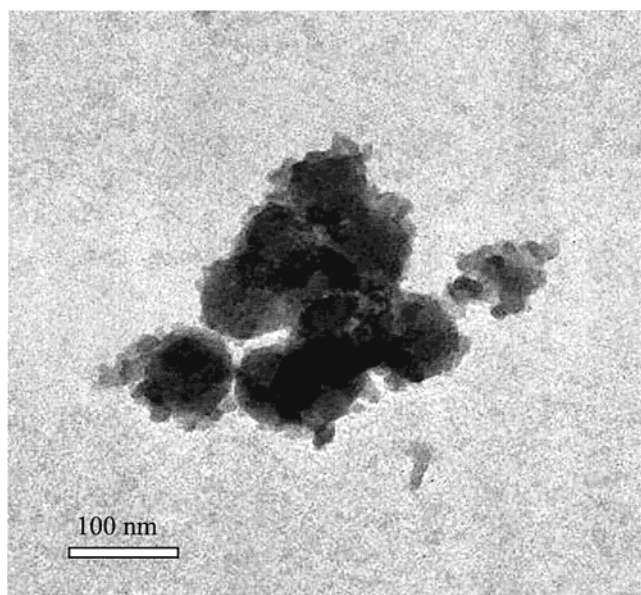


Figure 7. TEM image of polymer-IrO₂/SiO₂ system; polymer, 2.2×10^{-7} mol; IrO₂, 3.1×10^{-7} mol; SiO₂, 0.05 g.

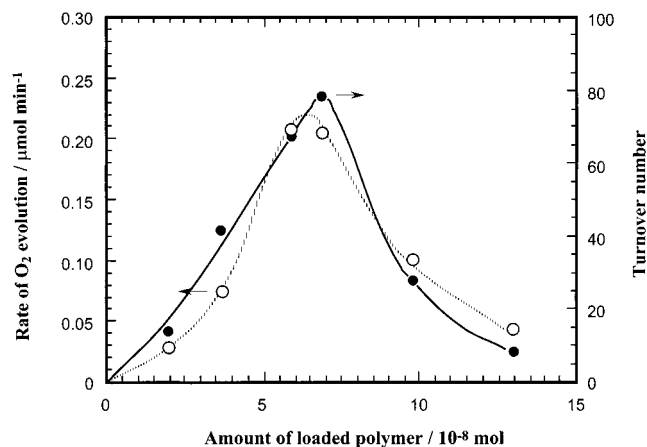


Figure 8. Dependence of the photocatalytic activity of polymer-IrO₂/SiO₂ system on the amount of adsorbed polymer; IrO₂, 3.1×10^{-7} mol; SiO₂, 0.05 g.

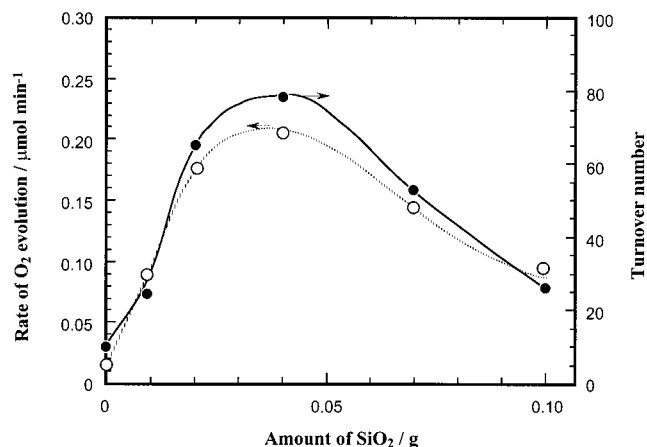


Figure 9. Dependence of the photocatalytic activity of polymer-IrO₂/SiO₂ system on SiO₂ support; polymer, 2.0×10^{-7} to 2.2×10^{-7} mol; IrO₂, 3.1×10^{-7} mol.

absorption by the large amount of adsorbed polymer. As shown in Figure 9, a sample prepared without the SiO₂ support has low activity compared with polymer-

IrO₂/SiO₂ or polymer-colloidal IrO₂ samples because of aggregation of the polymer during sample preparation. These results suggest that SiO₂ particles prevent the polymer-covered IrO₂ particles from aggregating and thereby prevent the loss of photocatalytic activity. In Figure 9, the addition of SiO₂ beyond 0.04 g reduces the activity. This is consistent with the idea that excess anionic SiO₂ support increases the polymer adsorption onto SiO₂ and therefore decreases polymer contact with IrO₂.

It is important to understand the characteristics of colloidal IrO₂ and the role of the Na₂SiF₆-NaHCO₃ buffer in making a comparison between heterogeneous photocatalysts. The activity of the polymer-IrO₂/SiO₂ system prepared in an unbuffered solution is very low even though the sample adsorbs a relatively large amount of the sensitizer polymer (2.8×10^{-8} mol). The polymer-colloidal IrO₂ system containing the same amounts of polymer and colloidal IrO₂ has activity that is several times higher. This implies that most of the polymer on the heterogeneous photocatalyst is adsorbed on SiO₂ and is not available for the reaction. On the other hand, the same preparation in Na₂SiF₆-NaHCO₃ buffer attaches colloidal IrO₂ particles covered with the aggregated polymer to the SiO₂ support, and this leads to a relatively high photocatalytic activity. In the case of the polymer/IrO₂/Keggin/SiO₂ samples prepared in Na₂SiF₆-NaHCO₃ solution, the high loading of the aggregated polymer does not result in high efficiency. TEM images of the low activity polymer-IrO₂/Keggin/SiO₂ samples and high activity polymer-IrO₂/SiO₂ samples are quite similar (Figures 5 and 7, respectively), but the microscopic distribution of components is apparently quite different. These results can be reasonably explained by the idea that the cationic Keggin ions bind the IrO₂ particles to the silica surface, in the case of the polymer/IrO₂/Keggin/SiO₂ samples, but that the photosensitizer polymer preferentially binds to SiO₂ rather than IrO₂.

Conclusions

A cationic polymer containing tris(4,4'-dialkyl-2,2'-bipyridyl)ruthenium groups linked by aliphatic spacers photocatalytically oxidizes water in the presence of colloidal IrO₂ in a pH 5.5–5.7 Na₂SiF₆-NaHCO₃ buffer. The quantum efficiency for O₂ evolution and O₂ yield of the polymer-colloidal IrO₂ system are smaller than those of the monomer tris(2,2'-bipyridyl)ruthenium complex-IrO₂ system because Na₂SiF₆-NaHCO₃ solution gradually aggregates the polymer.

With polymer-IrO₂/Keggin/SiO₂ and polymer-IrO₂/SiO₂ heterogeneous photocatalysts prepared in unbuffered solutions, the polymer is not significantly adsorbed onto IrO₂, and the photocatalytic activities are quite low. Preparation of these catalysts in the Na₂SiF₆-NaHCO₃ buffer substantially increases the loading by aggregation of the polymer, presumably through formation of anionic poly(silicate) or colloidal SiO₂ particles. The polymer/IrO₂/Keggin/SiO₂ composites prepared under these conditions show low activity because the amount of sensitizer polymer available for the reaction is actually small despite the total adsorbed amount being large. When the polymer and colloidal IrO₂ are adsorbed onto SiO₂ in Na₂SiF₆-NaHCO₃ solution, the colloidal

IrO_2 particles are covered with a sufficient amount of the aggregated polymer to give a photocatalytic activity comparable to that of the polymer–colloidal IrO_2 system. To our knowledge, this is the first example of a heterogeneous water oxidation photosystem containing a polymeric sensitizer. Polyanions or anionic inorganic sheets such as $\text{Zr}(\text{HPO}_4)_2 \cdot \text{H}_2\text{O}$ or HTiNbO_5 could, in principle, be adsorbed onto the surface of the cationic polymer– $\text{IrO}_2/\text{SiO}_2$ or polymer– $\text{IrO}_2/\text{SiO}_2$ composites and might serve to couple these photocatalysts to electron acceptors other than persulfate. Future work will focus on linking electron/energy transfer cascades,

grown layer-by-layer on these supports, to supported catalysts for oxygen evolution.

Acknowledgment. This work was supported by the Division of Chemical Sciences, Office of Basic Energy Sciences, Department of Energy, under Contract No. DE-FG02-93ER14374. We thank Dr. Rosemary Walsh and the Electron Microscope Facility for the Life Sciences in the Biotechnology Institute at Pennsylvania State University for the use of the transmission electron microscope.

CM0104811